© 2015. Published by The Company of Biologists Ltd | Development (2015) 142, 567-574 doi:10.1242/dev.114835

RESEARCH ARTICLE

A dynamic *Shh* expression pattern, regulated by SHH and BMP signaling, coordinates fusion of primordia in the amniote face

Diane Hu[1], Nathan M. Young[1], Xin Li[1,2], Yanhua Xu[1,3], Benedikt Hallgrímsson[4] and Ralph S. Marcucio[1,*]

ABSTRACT

The mechanisms of morphogenesis are not well understood, yet shaping structures during development is essential for establishing correct organismal form and function. Here, we examine mechanisms that help to shape the developing face during the crucial period of facial primordia fusion. This period of development is a time when the faces of amniote embryos exhibit the greatest degree of similarity, and it probably results from the necessity for fusion to occur to establish the primary palate. Our results show that hierarchical induction mechanisms, consisting of iterative signaling by Sonic hedgehog (SHH) followed by Bone morphogenetic proteins (BMPs), regulate a dynamic expression pattern of *Shh* in the ectoderm covering the frontonasal (FNP) and maxillary (MxP) processes. Furthermore, this *Shh* expression domain contributes to the morphogenetic processes that drive the directional growth of the globular process of the FNP toward the lateral nasal process and MxP, in part by regulating cell proliferation in the facial mesenchyme. The nature of the induction mechanism that we discovered suggests that the process of fusion of the facial primordia is intrinsically buffered against producing maladaptive morphologies, such as clefts of the primary palate, because there appears to be little opportunity for variation to occur during expansion of the *Shh* expression domain in the ectoderm of the facial primordia. Ultimately, these results might explain why this period of development constitutes a phylotypic stage of facial development among amniotes.

KEY WORDS: Frontonasal ectodermal zone, BMP, SHH, Cleft lip and palate, Craniofacial development, Facial fusion, Chick, Mouse

INTRODUCTION

Morphogenesis of the face is a complex process that involves iterative signaling between epithelial and mesenchymal cells. These interactions establish domains of directional growth that ultimately sculpt the face. An important morphogenetic event in facial development is the fusion of the maxillary (MxP), lateral nasal (LNP) and medial nasal (MNP) portion of the frontonasal process (FNP) to form the primary palate of the upper jaw. We have recently determined that a phylotypic stage exists, precisely around the time of fusion of the facial primordia (Young et al., 2014). At this time, the faces of amniote embryos exhibit the highest degree of morphological resemblance because, independent of the final adult form, they all pass through a developmental stage in which the facial buds collide and fuse to form the face (Young et al., 2014).

Signaling by Sonic hedgehog (Hu et al., 2003; Hu and Marcucio, 2009b; Young et al., 2010), Fibroblast growth factor (Richman et al., 1997; Szabo-Rogers et al., 2008, 2009; Griffin et al., 2013), Bone morphogenetic protein (Francis-West et al., 1994; Duprez et al., 1996; Ashique et al., 2002a,b; Foppiano et al., 2007) and Wnt (Brugmann et al., 2007; Geetha-Loganathan et al., 2009; Reid et al., 2011) all contribute to facial morphogenesis. Our work has focused primarily on the role of the frontonasal ectodermal zone (FEZ) during development of the upper jaw (Hu et al., 2003; Hu and Marcucio, 2009b). In amniotes, the FEZ is located in the stomodeal ectoderm and comprises a domain of *Shh*-expressing cells that line the roof of the mouth and a domain of *Fgf8*-expressing cells that covers the dorsal region of the FNP. Once *Shh* expression begins in the FEZ, *Fgf8* expression becomes restricted to the epithelium lining the nasal pits. Together, these and other molecules regulate the proximo-distal extension and dorso-ventral polarity of the upper jaw. However, the role of the FEZ on directing growth of the facial primordia during prominence fusion is unknown.

In this study, we have determined the relative movements of the MNP, LNP and MxP during their fusion. These tissue displacements are regulated by a series of epithelial-mesenchymal interactions, involving the FEZ and the neural crest mesenchyme. Signaling by the SHH and BMP pathways regulates the changing expression domain of *Shh* in the FEZ, which coordinates the directional growth of the facial buds required for the formation of the primary palate.

RESULTS

Integrated movement of the MNP toward the LNP and MxP

Our first goal was to assess the major trajectories of tissue displacement during development of the primary palate. Three-dimensional (3D) shape analysis of the face during normal morphogenesis demonstrates how the MNP, LNP and MxP follow orchestrated movements that result in distal contact and ultimately fusion. Specifically, when applied to an early-stage embryo, the shape vector associated with age shows that the MxP primarily grows in an anterior direction, whereas the MNP grows in a caudal (downward or posterior) direction with little initial anterior outgrowth (Fig. 1; supplementary material Movie 1). The globular process of the FNP and the lower margins of the nasal pits next meet at the distal tip of the MxP, an event associated with subsequent fusion of the prominences. After fusion, the avian FNP undergoes rapid expansion, associated with the derived proportions of the premaxilla and upper beak (Young et al., 2014).

Shh expression in the facial ectoderm is dynamic

In both chick (*Gallus gallus*) and mouse (*Mus musculus*) embryos, *Shh* is expressed in the surface cephalic ectoderm covering the roof of the stomodeum once neural crest cells arrive in the region (Hu and

[1]Department of Orthopaedic Surgery, San Francisco General Hospital, Orthopaedic Trauma Institute, The University of California at San Francisco, School of Medicine, San Francisco, CA 94110, USA. [2]National Key Laboratory of Bio-Macromolecule, Chinese Academy of Sciences, Beijing 100101, China. [3]Epitomizes, Inc., 1418 Moganshan Road, Hangzhou, Zhejiang 310011, China. [4]Department of Anatomy and Cell Biology, University of Calgary, McCaig Institute for Bone and Joint Health, Calgary, Alberta, Canada T2N 4N1.

*Author for correspondence (marcucio@orthosurg.ucsf.edu)

Received 27 June 2014; Accepted 5 December 2014

Development (2015) 142, 567-574 doi:10.1242/dev.114835

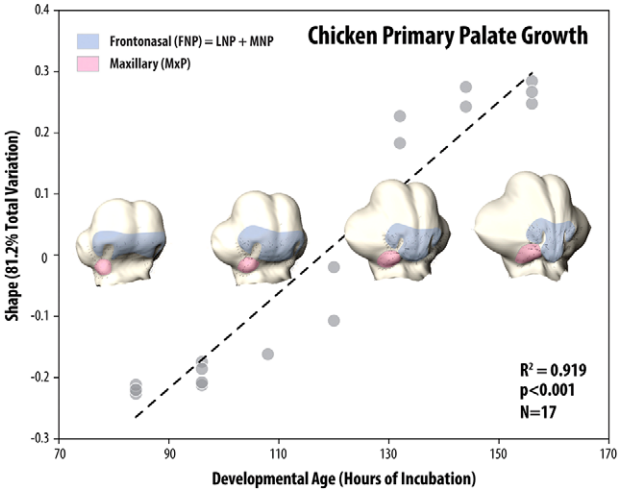

Fig. 1. Shape changes during morphogenesis of the upper jaw primordia. We performed a 3D morphometric analysis of facial shape changes during primary palate morphogenesis in the chicken. We applied homologous landmarks (n=20) to the embryonic craniofacial region (Young et al., 2014), performed a Procrustes superimposition to remove the effects of scale and orientation, and regressed the individual (n=17) shape coordinates against developmental age (hours of incubation) (r^2=0.919, explaining 81.1% total shape variation). To visualize shape changes associated with age, we next applied the associated shape-age vector to a representative 3D model of an early stage (84 h) embryo, and projected it to 160 h of development (i.e. +76 h). External surfaces associated with the FNP (blue) and MxP (red) were color-coded to enhance visualization and facilitate interpretation (see supplementary material Movie 1). Relative shape changes associated with increasing age include greater anterior projection of the FNP and maxillary, and a caudal (posterior) movement of the FNP. The relative narrowing and closer approximation of the nasal pits is partially due to the growth of surrounding tissues, i.e. the pits move less relative to the surrounding tissues such as the eyes, resulting in a shape in which they are closer together. The sum effect of these movements is for the maxillary and the globular process of the FNP approximating, contacting and then fusing at their distal margins to form an integrated primary palate and upper beak.

Marcucio, 2012). The *Shh* expression domain initially forms a boundary with ectodermal cells expressing *Fgf8*, but, once *Shh* is expressed, *Fgf8* is quickly downregulated and transcripts are restricted to the ectoderm of the nasal pits (Hu et al., 2003). In chicks, this occurs around Hamburger–Hamilton stages (HH) 20-21, and in mice, this occurs between embryonic day (E) 9.5 and E10.5 (Hu and Marcucio, 2009b). In both species, after *Fgf8* becomes restricted to the nasal pit, the *Shh* expression domain expands laterally into the maxillary process, the globular process of the FNP and into the nasal pit (Fig. 2A-D,F-I; n=12). After fusion, *Shh* expression is only detectable in the roof of the mouth (Fig. 2E,J; n=12).

SHH and BMP signaling work in series to regulate the expansion of *Shh*

The goal of our work was to assess the molecular mechanism(s) underlying the expansion of *Shh* expression in the surface ectoderm, and to determine the effect that this changing expression has on morphogenesis of the upper jaw. Our previous research has shown that both SHH and BMP signaling is required for the initial expression and maintenance of *Shh* expression in the FEZ (Foppiano et al., 2007; Hu and Marcucio, 2009a; Marcucio et al., 2011). Therefore, we wanted to assess the role of these two signaling pathways during expansion of the *Shh* expression domain.

To test the ability of SHH signaling to regulate *Shh* expression we performed gain- and loss-of-function experiments in chick embryos. First, we implanted beads soaked in SHH-N into one side of the FNP of chick embryos at HH 20 and assessed *Shh* expression 24 h later (~HH 23/24). *Shh* expression was strongly upregulated in the globular domain of the FNP on the treated side compared with the untreated side (Fig. 3A,B; n=12), and this was accompanied by increased cell proliferation (Fig. 3C-E). Controls, implanted with beads soaked in BSA showed no change in gene expression (Fig. 6A; n=10). In addition to changes in *Shh* expression, we also observed that Bmp2, 4 and 7 were significantly upregulated in these embryos [Fig. 3F; n=8; see also Hu and Helms (1999); Foppiano et al. (2007); Chong et al. (2012)].

Next, we electroporated a dominant-negative Ptc ($Ptc^{\Delta Loop2}$) into the ectoderm covering one side of the FNP at HH 15 (Fig. 4; n=35). We assessed SHH signaling in treated embryos using qPCR, and determined that, 48 h after electroporation (~HH 23/24), *Ptc* and *Gli1* expression levels were significantly downregulated (Fig. 4I; n=6), as was expression of *Shh* itself (Fig. 4I; n=8). Control embryos, electroporated with HSP-*lacZ* (Fig. 4A,B), showed no change in gene expression (Fig. 4C; supplementary material Fig. S1). The decreased *Shh* expression on the treated side was apparent by *in situ* hybridization (Fig. 4D; n=21). We observed similar outcomes when we blocked SHH signaling using the antagonist cyclopamine (supplementary material Fig. S2; n=30), and we did not observe evidence of apoptosis in the mesenchyme after blocking SHH with cyclopamine (supplementary material Fig. S3B,C; n=9). Additionally, *Fgf8* expression was not restricted to the nasal pits after blocking SHH signaling, thereby suggesting that SHH signaling is required for downregulation of *Fgf8* expression across the midline of the FNP (Fig. 4E,F; n=9). This agrees with previous publications (Cordero et al., 2004; Foppiano et al., 2007; Abzhanov et al., 2007). We observed no change in *Wnt9b* expression compared with normal embryos (Fig. 4G,H; n=9). *Bmp2* exhibited no change, whereas *Bmp4* and *Bmp7* were downregulated (Fig. 4J; n=6).

As we observed changes in *Bmp* expression levels associated with altered *Shh* expression, we wanted to assess the extent to which BMP signaling acts in concert with SHH signaling to regulate the expansion of *Shh* expression in the facial ectoderm. We blocked BMP signaling by implanting a bead soaked in Noggin protein into the mesenchyme on one side of the FNP of chick embryos at HH ~15/16. We then examined *Shh* expression 48 h later. We observed a significant decrease in *Shh* expression levels (Fig. 5E, qPCR; n=6). Whole-mount *in situ* hybridization confirmed that *Shh* expression was lost in the ectoderm on the treated side of the embryos (Fig. 5A-C; n=9), and there was a lack of outgrowth on that side of the embryo (Fig. 5B,C).

Our data suggest that SHH and BMP signaling work together to regulate the expansion of *Shh* expression within the facial ectoderm. We next wanted to determine whether SHH and BMP work in parallel or in succession to control expression of *Shh* in the ectoderm. First, we blocked BMP signaling by implanting a bead soaked in Noggin into one side of the FNP (HH ~15/16), and 24 h later we implanted a bead soaked in SHH-N. We observed that the *Shh* expression domain on the experimental side was absent (Fig. 5D; n=32), indicating that, after blocking BMP signaling, SHH was not able to restore the *Shh* expression pattern in the facial ectoderm. Next, we blocked SHH signaling by electroporating $Ptc^{\Delta Loop2}$ into the ectoderm at HH ~15/16, and 24 h later we placed a bead soaked in BMP4 into the mesenchyme on the experimental side. After 24 h we assessed *Shh* expression and determined that BMP signaling was able to restore *Shh* expression in the facial ectoderm (Fig. 6D; n=9).

Development (2015) 142, 567-574 doi:10.1242/dev.114835

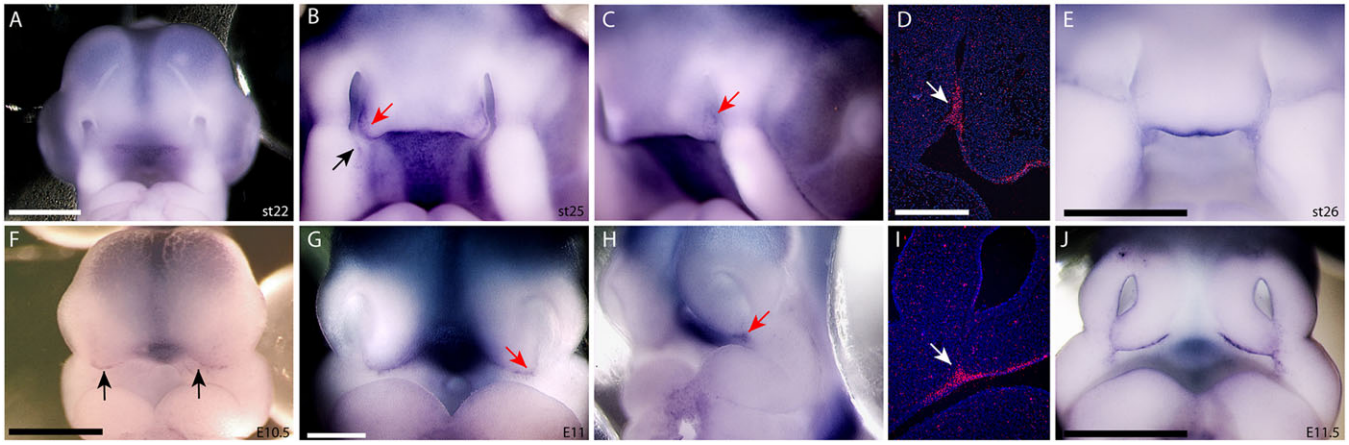

Fig. 2. Changes in *Shh* expression during morphogenesis of the upper jaw. (A) At HH 22, *Shh* expression is restricted to the ectoderm lining the roof of the stomodeum. (B) By HH 25, *Shh* expression has expanded into ectoderm covering the maxillary process (black arrow) and the globular process of the FNP (red arrow). (C) In lateral view and (D) in sections, expression of *Shh* in the nasal pit epithelium is also evident at HH 25. (E) By HH 26, *Shh* expression is restricted to the distal tip of the upper jaw. (F) In E10.5 mice, *Shh* expression is restricted to two domains in the MNP (black arrows). (G-I) By E11.0, *Shh* expression has expanded into the nasal pit epithelium (arrows). (J) By E11.5, *Shh* expression is restricted to paired bilateral expression domains in the distal part of the MNP. Scale bars: 1 mm in A for A-C, in E,F,J; 250 µm in D for D,I; 500 µm in G for G,H.

SHH signaling directs growth of the facial primordia during fusion of the primary palate

The expansion of the *Shh* expression domain into the globular process and nasal pit epithelium has not been described before, and we wanted to understand the functional significance of the expanded *Shh* expression domain on facial morphogenesis. We therefore repeated the loss-of-function experiments using $Ptc^{\Delta Loop2}$ and cyclopamine described above, and allowed embryos to develop to later stages for analysis. In all cases, we observed hypoplasia of the lateral edge of the FNP, a failure of the globular process to contact the lateral nasal and maxillary processes, and a cleft of the primary palate (Fig. 7; n=7; supplementary material Fig. S4; n=7). The treated side was smaller than the contralateral side (Fig. 7B versus Fig. 7D), and this hypoplasia was associated with decreased cell proliferation (supplementary material Fig. S2E,F; n=8) but not apoptosis (supplementary material Fig. S3; n=8).

In addition to the loss-of-function experiments, we also activated SHH signaling in the globular process and assessed the morphological outcomes at later time points. We observed that the direction of growth of the lateral regions of the FNP was altered (supplementary material Fig. S5; n=6). Instead of arching laterally to extend and touch the lateral nasal and maxillary processes, the FNP grew rostrally and did not meet with the other facial primordia, and the treated side was longer and broader than the contralateral side. The result of this aberrant growth was the formation of a cleft of the primary palate (supplementary material Fig. S5; n=6). In this case, the morphological changes were associated with increased cell proliferation and the affected region was larger (Fig. 3; n=8).

DISCUSSION

Morphogenesis is a complex process in which 3D shape is generated *de novo* during embryogenesis. Although many advances have been made regarding the signaling interactions that control histogenesis, how these signaling interactions regulate morphogenesis are not well studied. A recent report indicated that, during morphogenesis of the upper jaw, SHH signaling participates in regulating the balance between proliferation and apoptosis, which is required for proper growth of the facial primordia and for fusion and dissolution of the epithelial seam during fusion of the facial primordia (Kurosaka et al., 2014). The entire process of fusion is molecularly complex, and is regulated in part by the interactions of Pbx, Wnt, Irf6 and p63 (Thomason et al., 2010; Ferretti et al., 2011). Here, we focused on the mechanisms that regulate the changing pattern of expression of *Shh* changes during fusion of the facial primordia. Our results show that an iterative series of signals between the ectoderm and mesenchyme of the face orchestrate the changing expression pattern of *Shh* in the FEZ. This changing pattern of *Shh* regulates the morphogenetic movements that lead to the formation of the primary palate by coordinating the shape changes of the MNP, LNP and MxP in order for fusion of the primordia to occur.

Mechanisms of morphogenesis

The nature of the morphogenetic movements that generate the shape changes during fusion of the primary palate is unknown. Previous models have relied on location of differential zones of proliferation as mediators of shape change and morphogenesis (Ede et al., 1975; Wu et al., 2006). Our work here supports a role for changes in proliferation driving the morphogenetic process, but simple changes in the rate or location of proliferating cells is unlikely to underlie all of the directional growth that is observed during facial development. Morphogenesis of epithelially derived structures results from cellular changes that involve shape changes and polarized activities (Guillot and Lecuit, 2013). A recent study on hair follicles has shown that movements of epithelial cells, but not cell proliferation, were responsible for shaping the follicle (Ahtiainen et al., 2014). The relevance of directed cell behaviors in morphogenesis is not restricted to the epithelium. Studies on the limb have shown that non-directional growth alone is unable to explain the shape changes the limb bud experiences during development. Rather, polarized cell activities, such as cell movement in the mesenchyme, appear to comprise the emergent properties that generate shape (Boehm et al., 2010; Hopyan et al., 2011). Results from work in our laboratory indicate that polarized cellular behaviors associated with cell movement are associated with facial shape (Li et al., 2013). In a multi-primordia organ like the upper jaw, the influence of these cellular behaviors on interactions among the facial primordia would also contribute to overall jaw morphology (Linde-Medina and Newman, 2014). Together, these results suggest that cell movements generate forces

Development (2015) 142, 567-574 doi:10.1242/dev.114835

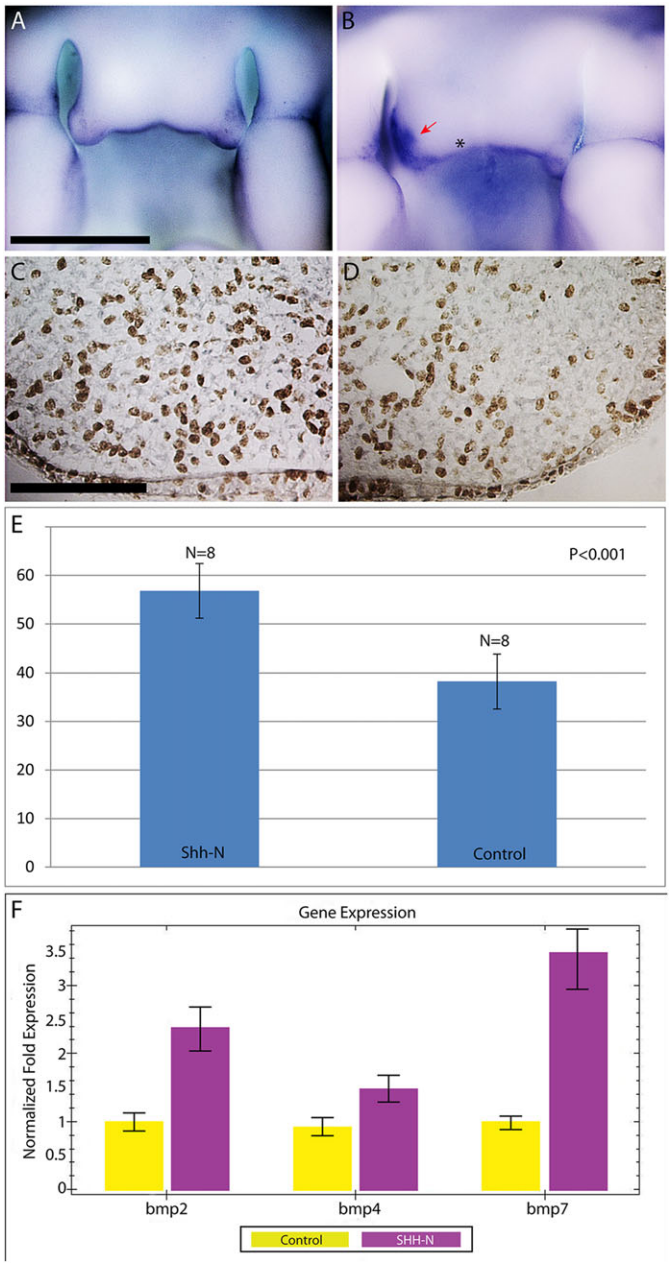

Fig. 3. Activating the Hh pathway increases Shh expression in the FNP. (A) At HH 25, *Shh* expression is observed in the FEZ. (B) After treatment with SHH-N, *Shh* expression is strongly upregulated in the ectoderm covering the globular process on the treated side (red arrow). The asterisk marks the location of the bead. (C) Representative section showing BrdU incorporation on the treated side and (D) on the contralateral side of the same embryo. (E) Cell proliferation is significantly increased on the treated side of the embryo ($P<0.05$). Error bars indicate s.e.m. (F) After SHH treatment, *Bmp2* ($P=0.019$), *Bmp4* ($P=0.086$) and *Bmp7* ($P=0.025$) were upregulated in the mesenchyme. Error bars indicate s.e.m. Scale bars: 1 mm in A for A,B; 100 µm in C for C,D.

within the mesenchymal tissues that drive morphogenetic processes. Further work is required to directly test this hypothesis in facial morphogenesis.

SHH and BMP form a signaling loop in the craniofacial complex

SHH and BMP signaling are essential for proper development of the face. BMP signaling is directly or indirectly involved in the regulation of the onset of *Shh* expression in the FEZ at HH 20 (Foppiano et al., 2007). Subsequently, SHH from the ectoderm appears to regulate the expression patterns of BMPs in the adjacent mesenchyme (Hu and Marcucio, 2009b). Our data show that, in turn, BMP signaling in combination with SHH itself regulate the expansion of the *Shh* domain into the epithelium of the nasal pits, maxillary processes and globular processes. However, our experiments do not reveal whether these regulatory interactions are direct. That is, whether SHH directly activates the *Bmp4* and *Bmp7* loci, and whether BMPs directly activate the *Shh* locus, are not known. Previously, a bead soaked in SHH protein was shown to activate expression of *Bmp4* in the mesenchyme of the FNP (Hu and Helms, 1999). Moreover, work by other investigators has revealed that *Bmp2* has a Gli2 response element that mediates Shh induction of *Bmp2* expression in osteoblasts (Zhao et al., 2006) and in the limb bud (Vokes et al., 2008). We are currently exploring the transcriptional interactions of these pathways during development of the FNP. Nonetheless, our results contradict previous research in which it was proposed that the ability of Noggin to block BMP signaling was responsible for the regulation of *Shh* expression in the facial ectoderm (Ashique et al., 2002a; Lana-Elola et al., 2011). These studies did not take into account that the *Shh* expression domain changes over time and that it eventually occupies new ectodermal regions during the directional growth of upper jaw primordia, a developmental event in which SHH signaling comes to play.

Our data demonstrate that SHH and BMP signaling act in succession to regulate the dynamic expression of *Shh* in the facial epithelium during morphogenesis. However, variation in SHH and BMP signaling does not appear to alter the positioning of the Shh expression domains. For example, gain-of-function experiments using SHH intensified *Shh* expression in the epithelial domains but did not lead to ectopic *Shh* expression or an expansion of the primary domain. This suggests that the ectodermal domains that express *Shh* acquire a competence prior to the onset of *Shh* expression and that the regulation of the spatio-temporal configuration of *Shh* expression in the FEZ is separate and distinct from the regulation of the level of *Shh* expression. For example, *Shh* expression in the unique domains of ectoderm is probably programmed by tissue-specific regulatory regions within the *Shh* locus. However, enhancer elements that drive *Shh* expression in the facial ectoderm remain unknown (Epstein et al., 1999, 2000; Jeong and Epstein, 2003; Jeong et al., 2006, 2008; Marcucio et al., 2011; Anderson et al., 2014).

This finding is in contrast to the observed pattern of *Shh* expression in the rugae (a series of epithelial ridges on the palate), where a Turing-type mechanism of activator-repressor interactions regulates the sequential onset of *Shh* expression in each rugal domain (Economou et al., 2012). In the palatal epithelium, ectopic *Shh* expression is observed when the activator-repressor mechanism is disrupted, as, for example, when a rugal domain is excised, eliminating the inhibitory molecules secreted by these cells. In this scenario, the expression domains arise from emergent inductive processes. If a similar mechanism functioned in the FEZ, then, by changing the steepness of the activator-repressor gradient in gain- and loss-of-function experiments, new *Shh* expression domains would appear, due to altered threshold responses within the ectoderm. Instead, we observed that the *intensity* of *Shh* expression changed, but the location of the domains remained unaltered. In this case, the inductive mechanisms underlying the new *Shh* expression domains appear to obey hierarchical principles as previously described (Salazar-Ciudad et al., 2003).

Development (2015) 142, 567-574 doi:10.1242/dev.114835

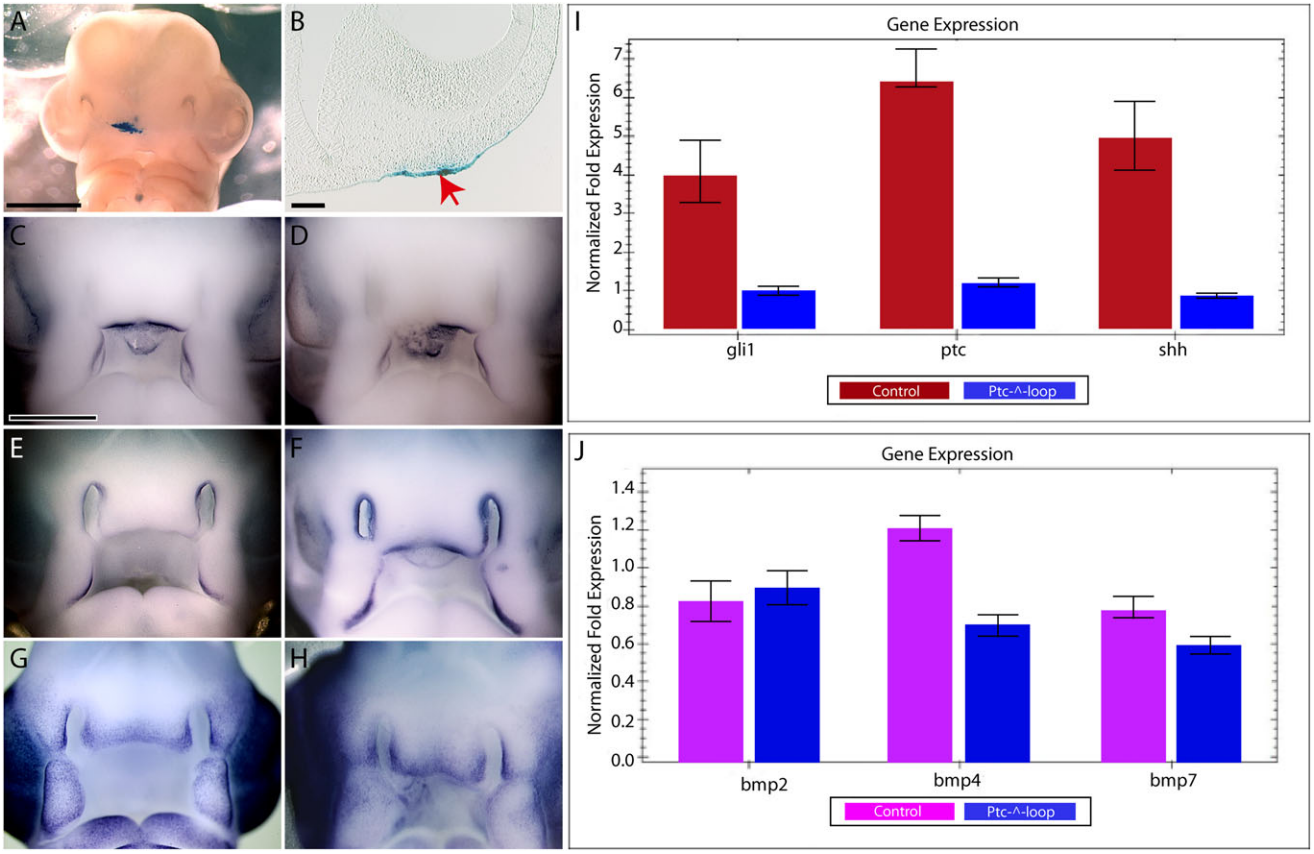

Fig. 4. Blocking SHH signaling inhibits expansion of *Shh* expression. (A,B) Electroporation of HSP-*lacZ* illustrates that the ectoderm is specifically targeted. (arrow in B). (C) *Shh* expression in control and (D) treated embryos. *Shh* expression does not expand into the nasal pit or globular process on the side electroporated with $Ptc^{\Delta Loop2}$. (E) *Fgf8* expression in control and (F) treated embryo shows that blocking SHH signaling leads to maintenance of *Fgf8* expression across the midline. (G) *Wnt9b* in control and (H) treated embryos shows no change in *Wnt9b* expression after blocking SHH signaling. (I) qPCR illustrates that *Shh* (P=0.013) and the downstream targets *Ptc* (P=0.021) and *Gli1* (P=0.018) are significantly reduced after electroporation of $Ptc^{\Delta Loop2}$. Error bars indicate s.e.m. (J) Similarly, *Bmp4* (P=0.038) and *Bmp7* (P=0.078) expression levels were decreased in embryos after blocking SHH signaling, whereas and *Bmp2* expression was unchanged at this time (P=0.129). Error bars indicate s.e.m. Scale bars: 1 mm in A,C-H; 400 µm in B.

Interestingly, a similar phenomenon is observed during the initial formation of the FEZ. We determined that SHH signaling within the brain (Marcucio et al., 2005; Hu and Marcucio, 2009a) and BMP signaling within the FNP (Foppiano et al., 2007) and the neural crest cells (Hu and Marcucio, 2012) act together to induce *Shh* expression in the ectoderm, thus giving rise to the formation of the FEZ. However, in our experiments, we never observed ectopic expression of *Shh* in the ectoderm, suggesting that the signals and cells appear to trigger a gene expression pattern that is inherent within the ectoderm itself. To date, the mechanisms underlying this phenomenon are unknown.

Relationship of shape to normal and diseased phenotypes

The inability to establish ectopic domains of *Shh* expression or deviate significantly from the anatomical configuration of the FEZ during formation of the primary palate reflects the constraint placed on facial shape during this period of development. We have shown in a large comparative analysis of the development of the amniote face that a phylotypic stage exists around the time of palatal fusion (Young et al., 2014). At this time, facial shapes among amniotes converge in order for the primary palate to form, and after that, the faces are able to diverge into the array of morphologies present in adult amniotes. Our results suggest that spatial stability of the *Shh* expression domain in the facial ectoderm is a central feature of this constraint on variation during primary palate formation. Therefore, understanding how the *Shh* expression domain is stabilized is crucial for unraveling the mechanistic basis for the minimization of morphological variation both within and among species during the formation of the face. Our results show that, whereas the level of *Shh* expression is dynamically regulated by SHH and BMP signaling, the spatial domain of the FEZ is not. Instead, other pathways or mechanisms must act to stabilize the spatial domain of the FEZ during the formation of the face. This mechanistic separation of the spatial domain of FEZ expression and regulation of the level of *Shh* expression in the FEZ helps to explain the reduction in morphological variation during facial prominence fusion. Our results have revealed that levels of SHH and BMP signaling are important for proper development. For example, when we activated or suppressed the SHH pathway the resulting embryos produced clefts due to either hypo- or hyperplasia of the affected primordia. This agrees with our previous work, showing that shape is highly associated with successful fusion of the facial primordia. We propose that the resilience of the FEZ spatial expression domain contributes to the reduced shape variance observed at the time of prominence fusion among amniotes, as well as the high resilience to clefting phenotypes during development, but above or below a threshold of SHH signaling shapes can be generated that produce clefts.

In summary, we have determined that *Shh* expression in the facial ectoderm is dynamic. The expression domain unfolds in a very precise way as development proceeds, and the changing pattern of expression is regulated by a series of SHH and BMP

Development (2015) 142, 567-574 doi:10.1242/dev.114835

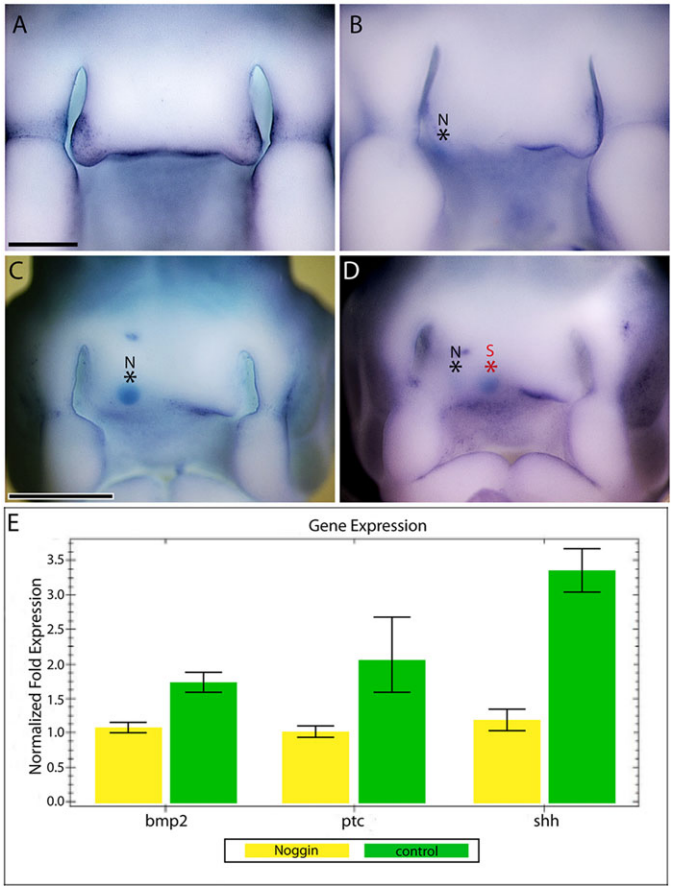

Fig. 5. Blocking BMP signaling inhibits expansion of *Shh* expression. (A) *Shh* expression in normal embryos (see Fig. 6A for control embryos) and (B,C) in embryos treated with Noggin. Noggin prevents the expansion of the *Shh* expression domain into the globular process and nasal pit epithelium (N* shows the location of the Noggin-soaked bead). (D) The *Shh* expression domain cannot be restored by placing a bead soaked in SHH-N (S* shows the location of the SHH-soaked bead) after blocking BMP signaling with a Noggin bead. (E) After blocking BMP signaling, *Bmp2* (P=0.047), *Shh* (P=0.028) and *Ptc* (P=0.038) expression levels were all decreased. Error bars indicate s.e.m. Scale bars: 0.5 mm in A for A,B; 1 mm in C for C,D.

signaling events. The role of SHH in promoting fusion of the facial primordia is essential for proper facial morphogenesis (Kurosaka et al., 2014). Understanding the precise mechanisms by which the *Shh* expression domain is positioned within the ectoderm will be a key step in understanding the molecular mechanisms that regulate morphogenesis of the upper jaw.

MATERIALS AND METHODS

Embryo preparation

Chick embryos were incubated at 39°C until either collection or experimentation. For FEZ analysis, chick embryos were harvested at HH 22, HH 25 and HH 26, and mouse embryos were harvested at E10.5, E11 and E11.5. Alternatively, chick embryos were prepared for surgery as described (Hu and Marcucio, 2011). All embryos were fixed in 4% paraformaldehyde, dehydrated in a graded series of methanol and stored at −20°C until analysis. The experiments conform to institutional and national regulatory standards that are applied for analysis of vertebrate embryos.

Preparation and placement of beads

Affi-Gel Blue beads (70-140 mesh, 100-200 µm diameter; Bio-Rad) were rinsed four times in PBS and manually selected for uniform size. Beads were soaked in 0.1% bovine serum albumin (BSA), recombinant human BMP4 (4 µg/ml with 0.1% BSA; R&D Systems), recombinant human Noggin-N (250 µg/ml with 0.1% BSA; R&D Systems) or recombinant SHH-N (400 µg/ml with 0.1% BSA; Ontogeny) for ≥1 h at 37°C. Prior to initiating experiments, we performed a dose-response experiment for BMP4 to determine a dose that did not induce apoptosis. Protein-soaked beads were stored at 4°C for a maximum of 1 week. Beads were placed into the right side of the FNP by accessing the face as described (Hu and Marcucio, 2011).

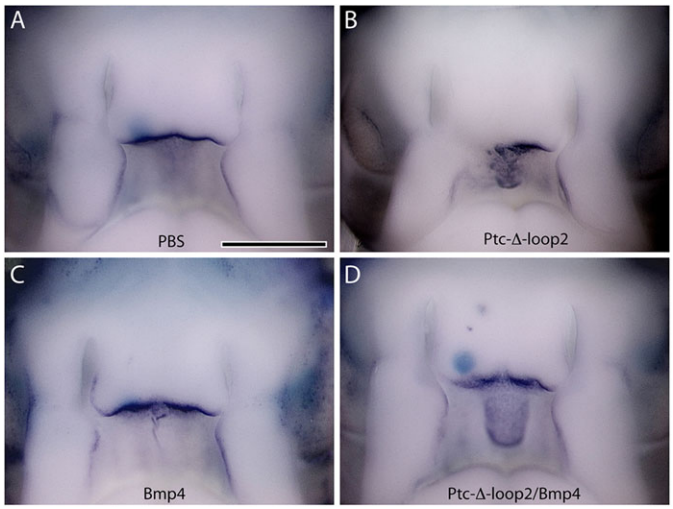

Fig. 6. BMPs appear to act downstream of SHH in regulating the expansion of *Shh* expression. (A) *Shh* expression in a control embryo (0.1% BSA-soaked beads; n=10), and (B) the reduction of *Shh* expression after blocking SHH signaling. (C) A bead soaked in BMP4 does not affect *Shh* expression or facial morphology. (D) A bead soaked in BMP4 restores *Shh* expression after blocking SHH signaling by electroporating $Ptc^{\Delta Loop2}$. Scale bar: 1 mm.

Electroporation

$Ptc^{\Delta Loop2}$ [see Briscoe et al. (2001), concentration 3 µg/µl] or HSP-*lacZ* (concentration 3 µg/µl) were injected beneath the head at HH 15/16 and electroporated into the ectoderm using an Intracel TSS20 Ovodyne Electroporator (10 V, 5 pulses, pulse width=20).

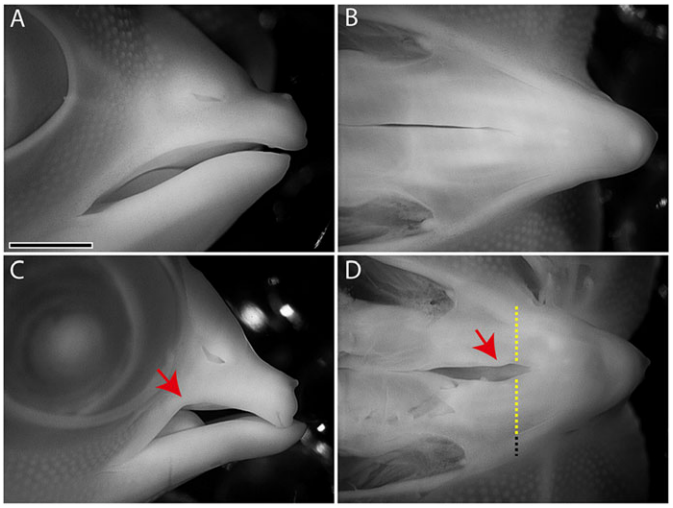

Fig. 7. Blocking SHH signaling leads to cleft palate. (A) Lateral and (B) ventral view of a normal chick embryo at day 10. (C) Lateral and (D) ventral view of an embryo after blocking SHH signaling illustrates the cleft of the primary palate (red arrow in C) and a widening of the gap in the secondary palate (red arrow in D). The treated side is reduced in size. The dotted yellow line shows the size of the treated side of the upper jaw, and the combined dotted yellow and black lines indicate the normal size. Scale bar: 2 mm.

Development (2015) 142, 567-574 doi:10.1242/dev.114835

Geometric morphometrics

We collected chicken embryos (n=17) spanning the time period of initial facial morphogenesis (84-160 h of incubation), from initial prominence outgrowth through primary palate fusion. We scanned each embryo in a µCT 40 micro-CT scanner (Scanco) at a resolution of 12-20 µm. Reconstructed image stacks were converted into 3D objects in Amira 5.4 (Visage Imaging) and surfaces were landmarked in Landmark Editor 3.0 (Institute for Data Analysis and Visualization) (n=20). We next imported the raw coordinates into MorphoJ (Klingenberg, 2011), and performed a Procrustes superimposition to minimize differences in orientation and scale. We next performed a multivariate regression of the Procrustes coordinates on age (hours of incubation), and utilized the resulting age-shape vector to project a representative early stage embryo (84 h) to 160 h of development.

BrdU labeling and TUNEL

Twenty minutes prior to collection, 200 nl of bromodeoxyuridine (BrdU) labeling reagent (Invitrogen) was injected into the vitelline vein. Embryos were fixed, embedded and sectioned as described. BrdU-labeled cells were visualized on paraffin sections; detection of BrdU incorporation was assessed by immunohistochemistry following the manufacturer's instructions (Invitrogen). BrdU-incorporated cells were counted (Olympus) and the percentage of proliferating cells in the medial portion of the FNP was determined. Student's t-test was performed to determine statistical significance (P<0.05). A terminal deoxynucleotidyl transferase dUTP nick end labeling (TUNEL) assay was performed according the manufacturer's instructions (Roche).

In situ hybridization

In situ hybridization was performed on paraffin sections and whole embryos as described (Albrecht et al., 1997). Subclones of chick *Shh*, *Wnt9b*, *Fgf8* and mouse *Shh* were linearized to transcribe digoxygenin-labeled antisense riboprobes. For whole mounts, tissues were hybridized with 0.5-1 µg/ml digoxygenin-labeled cRNA probes, and, after washing, were incubated with an alkaline phosphatase-conjugated anti-digoxygenin antibody (Boehringer). NBT/BCIP substrate (Roche) was used for color detection. For *in situ* hybridization on sections, tissues were hybridized with ^{35}S-labeled cRNA, washed, air-dried and coated with liquid emulsion (Kodak). The *in situ* hybridization signal was visualized as described previously (Albrecht et al., 1997).

Total RNA preparation and qPCR

The FNP of embryos was dissected and subjected to 2 mg/ml dispase digestion on ice for 20 min. Neural ectoderm was separated from the surface ectoderm and mesenchyme using tungsten needles. Ectoderm and mesenchyme from individual embryos were used to create mRNA. RNA samples were isolated using an mRNeasy Kit (Qiagen). cDNA synthesis used Invitrogen Superscript III following the manufacturer's instructions. qPCR was performed using a Bio-Rad CFX96 real-time PCR machine. qPCR primers for specific genes are listed in supplementary material Table S1. Relative gene expression was calculated based on the $2^{-\Delta Ct}$ method. ΔC_t was calculated between each target gene and *Gapdh* as control. At least three biological replicates were prepared for all analyses and Student's t-test was used to assess significance.

Acknowledgements

$Ptc^{\Delta Loop2}$ was a gift from Gary Struhl. We would like to thank all of the members of the Orthopaedic Trauma Institute, especially Gina Baldoza for constant support and Marta Linde for critical comments on the manuscript.

Competing interests

The authors declare no competing or financial interests.

Author contributions

D.H. and R.S.M. designed the research and conceived the experiments. D.H. performed all experimental manipulations. D.H., X.L., Y.X. and N.Y. collected the data. All authors analyzed the data and contributed to writing the paper.

Funding

This research was funded by the National Institutes of Health/National Institute of Dental and Craniofacial Research (NIH/NIDCR) [5R01-DE019638 to R.S.M. and B.H.; 2R01-DE018234 to R.S.M.]. Deposited in PMC for release after 12 months.

Supplementary material

Supplementary material available online at
http://dev.biologists.org/lookup/suppl/doi:10.1242/dev.114835/-/DC1

References

Abzhanov, A., Cordero, D. R., Sen, J., Tabin, C. J. and Helms, J. A. (2007). Cross-regulatory interactions between Fgf8 and Shh in the avian frontonasal prominence. *Congenit. Anom.* **47**, 136-148.

Ahtiainen, L., Lefebvre, S., Lindfors, P. H., Renvoisé, E., Shirokova, V., Vartiainen, M. K., Thesleff, I. and Mikkola, M. L. (2014). Directional cell migration, but not proliferation, drives hair placode morphogenesis. *Dev. Cell* **28**, 588-602.

Albrecht, U. E. G., Helms, J. A. and Lin, H. (1997). Visualization of gene expression patterns by in situ hybridization. In *Molecular and Cellular Methods in Developmental Toxicology* (ed. G. P. Daston), pp. 24-48. Boca Raton, FL: CRC Press.

Anderson, E., Devenney, P. S., Hill, R. E. and Lettice, L. A. (2014). Mapping the Shh long-range regulatory domain. *Development* **141**, 3934-3943.

Ashique, A. M., Fu, K. and Richman, J. M. (2002a). Endogenous bone morphogenetic proteins regulate outgrowth and epithelial survival during avian lip fusion. *Development* **129**, 4647-4660.

Ashique, A. M., Fu, K. and Richman, J. M. (2002b). Signalling via type IA and type IB bone morphogenetic protein receptors (BMPR) regulates intramembranous bone formation, chondrogenesis and feather formation in the chicken embryo. *Int. J. Dev. Biol.* **46**, 243-253.

Boehm, B., Westerberg, H., Lesnicar-Pucko, G., Raja, S., Rautschka, M., Cotterell, J., Swoger, J. and Sharpe, J. (2010). The role of spatially controlled cell proliferation in limb bud morphogenesis. *PLoS Biol.* **8**, e1000420.

Briscoe, J., Chen, Y., Jessell, T. M. and Struhl, G. (2001). A hedgehog-insensitive form of patched provides evidence for direct long-range morphogen activity of sonic hedgehog in the neural tube. *Mol Cell.* **7**, 1279-1291.

Brugmann, S. A., Goodnough, L. H., Gregorieff, A., Leucht, P., ten Berge, D., Fuerer, C., Clevers, H., Nusse, R. and Helms, J. A. (2007). Wnt signaling mediates regional specification in the vertebrate face. *Development* **134**, 3283-3295.

Chong, H. J., Young, N. M., Hu, D., Jeong, J., McMahon, A. P., Hallgrimsson, B. and Marcucio, R. S. (2012). Signaling by SHH rescues facial defects following blockade in the brain. *Dev. Dyn.* **241**, 247-256.

Cordero, D., Marcucio, R., Hu, D., Gaffield, W., Tapadia, M. and Helms, J. A. (2004). Temporal perturbations in sonic hedgehog signaling elicit the spectrum of holoprosencephaly phenotypes. *J. Clin. Invest.* **114**, 485-494.

Duprez, D., Bell, E. J. d. H., Richardson, M. K., Archer, C. W., Wolpert, L., Brickell, P. M. and Francis-West, P. H. (1996). Overexpression of BMP-2 and BMP-4 alters the size and shape of developing skeletal elements in the chick limb. *Mech. Dev.* **57**, 145-157.

Economou, A. D., Ohazama, A., Porntaveetus, T., Sharpe, P. T., Kondo, S., Basson, M. A., Gritli-Linde, A., Cobourne, M. T. and Green, J. B. A. (2012). Periodic stripe formation by a Turing mechanism operating at growth zones in the mammalian palate. *Nat. Genet.* **44**, 348-351.

Ede, D. A., Flint, O. P. and Teague, P. (1975). Cell proliferation in the developing wing-bud of normal and talpid3 mutant chick embryos. *J. Embryol. Exp. Morphol.* **34**, 589-607.

Epstein, D. J., McMahon, A. P. and Joyner, A. L. (1999). Regionalization of Sonic hedgehog transcription along the anteroposterior axis of the mouse central nervous system is regulated by Hnf3-dependent and -independent mechanisms. *Development* **126**, 281-292.

Epstein, D. J., Martinu, L., Michaud, J. L., Losos, K. M., Fan, C. and Joyner, A. L. (2000). Members of the bHLH-PAS family regulate Shh transcription in forebrain regions of the mouse CNS. *Development* **127**, 4701-4709.

Ferretti, E., Li, B., Zewdu, R., Wells, V., Hebert, J. M., Karner, C., Anderson, M. J., Williams, T., Dixon, J., Dixon, M. J. et al. (2011). A conserved Pbx-Wnt-p63-Irf6 regulatory module controls face morphogenesis by promoting epithelial apoptosis. *Dev. Cell* **21**, 627-641.

Foppiano, S., Hu, D. and Marcucio, R. S. (2007). Signaling by bone morphogenetic proteins directs formation of an ectodermal signaling center that regulates craniofacial development. *Dev. Biol.* **312**, 103-114.

Francis-West, P. H., Tatla, T. and Brickell, P. M. (1994). Expression patterns of the bone morphogenetic protein genes Bmp-4 and Bmp-2 in the developing chick face suggest a role in outgrowth of the primordia. *Dev. Dyn.* **201**, 168-178.

Geetha-Loganathan, P., Nimmagadda, S., Antoni, L., Fu, K., Whiting, C. J., Francis-West, P. and Richman, J. M. (2009). Expression of WNT signalling pathway genes during chicken craniofacial development. *Dev. Dyn.* **238**, 1150-1165.

Griffin, J. N., Compagnucci, C., Hu, D., Fish, J., Klein, O., Marcucio, R. and Depew, M. J. (2013). Fgf8 dosage determines midfacial integration and polarity within the nasal and optic capsules. *Dev. Biol.* **374**, 185-197.
Guillot, C. and Lecuit, T. (2013). Mechanics of epithelial tissue homeostasis and morphogenesis. *Science* **340**, 1185-1189.
Hopyan, S., Sharpe, J. and Yang, Y. (2011). Budding behaviors: growth of the limb as a model of morphogenesis. *Dev. Dyn.* **240**, 1054-1062.
Hu, D. and Helms, J. A. (1999). The role of sonic hedgehog in normal and abnormal craniofacial morphogenesis. *Development* **126**, 4873-4884.
Hu, D. and Marcucio, R. S. (2009a). A SHH-responsive signaling center in the forebrain regulates craniofacial morphogenesis via the facial ectoderm. *Development* **136**, 107-116.
Hu, D. and Marcucio, R. S. (2009b). Unique organization of the frontonasal ectodermal zone in birds and mammals. *Dev. Biol.* **325**, 200-210.
Hu, D. and Marcucio, R. S. (2011). Assessing signaling properties of ectodermal epithelia during craniofacial development. *J. Vis. Exp.* **49**, 2557.
Hu, D. and Marcucio, R. S. (2012). Neural crest cells pattern the surface cephalic ectoderm during FEZ formation. *Dev. Dyn.* **241**, 732-740.
Hu, D., Marcucio, R. S. and Helms, J. A. (2003). A zone of frontonasal ectoderm regulates patterning and growth in the face. *Development* **130**, 1749-1758.
Jeong, Y. and Epstein, D. J. (2003). Distinct regulators of Shh transcription in the floor plate and notochord indicate separate origins for these tissues in the mouse node. *Development* **130**, 3891-3902.
Jeong, Y., El-Jaick, K., Roessler, E., Muenke, M. and Epstein, D. J. (2006). A functional screen for sonic hedgehog regulatory elements across a 1 Mb interval identifies long-range ventral forebrain enhancers. *Development* **133**, 761-772.
Jeong, Y., Leskow, F. C., El-Jaick, K., Roessler, E., Muenke, M., Yocum, A., Dubourg, C., Li, X., Geng, X., Oliver, G. et al. (2008). Regulation of a remote Shh forebrain enhancer by the Six3 homeoprotein. *Nat. Genet.* **40**, 1348-1353.
Klingenberg, C. P. (2011). MorphoJ: an integrated software package for geometric morphometrics. *Mol. Ecol. Res.* **11**, 353-357.
Kurosaka, H., Iulianella, A., Williams, T. and Trainor, P. A. (2014). Disrupting hedgehog and WNT signaling interactions promotes cleft lip pathogenesis. *J. Clin. Invest.* **124**, 1660-1671.
Lana-Elola, E., Tylzanowski, P., Takatalo, M., Alakurtti, K., Veistinen, L., Mitsiadis, T. A., Graf, D., Rice, R., Luyten, F. P. and Rice, D. P. (2011). Noggin null allele mice exhibit a microform of holoprosencephaly. *Hum. Mol. Genet.* **20**, 4005-4015.
Li, X., Young, N. M., Tropp, S., Hu, D., Xu, Y., Hallgrimsson, B. and Marcucio, R. S. (2013). Quantification of shape and cell polarity reveals a novel mechanism underlying malformations resulting from related FGF mutations during facial morphogenesis. *Hum. Mol. Genet.* **22**, 5160-5172.
Linde-Medina, M. and Newman, S. (2014). Limb, tooth, beak: three modes of development and evolutionary innovation of form. *J. Biosci.* **39**, 211-223.
Marcucio, R. S., Cordero, D. R., Hu, D. and Helms, J. A. (2005). Molecular interactions coordinating the development of the forebrain and face. *Dev. Biol.* **284**, 48-61.
Marcucio, R. S., Young, N. M., Hu, D. and Hallgrimsson, B. (2011). Mechanisms that underlie co-variation of the brain and face. *Genesis* **49**, 177-189.
Reid, B. S., Yang, H., Melvin, V. S., Taketo, M. M. and Williams, T. (2011). Ectodermal Wnt/beta-catenin signaling shapes the mouse face. *Dev. Biol.* **349**, 261-269.
Richman, J. M., Herbert, M., Matovinovic, E. and Walin, J. (1997). Effect of fibroblast growth factors on outgrowth of facial mesenchyme. *Dev. Biol.* **189**, 135-147.
Salazar-Ciudad, I., Jernvall, J. and Newman, S. A. (2003). Mechanisms of pattern formation in development and evolution. *Development* **130**, 2027-2037.
Szabo-Rogers, H. L., Geetha-Loganathan, P., Nimmagadda, S., Fu, K. K. and Richman, J. M. (2008). FGF signals from the nasal pit are necessary for normal facial morphogenesis. *Dev. Biol.* **318**, 289-302.
Szabo-Rogers, H. L., Geetha-Loganathan, P., Whiting, C. J., Nimmagadda, S., Fu, K. and Richman, J. M. (2009). Novel skeletogenic patterning roles for the olfactory pit. *Development* **136**, 219-229.
Thomason, H. A., Zhou, H., Kouwenhoven, E. N., Dotto, G.-P., Restivo, G., Nguyen, B.-C., Little, H., Dixon, M. J., van Bokhoven, H. and Dixon, J. (2010). Cooperation between the transcription factors p63 and IRF6 is essential to prevent cleft palate in mice. *J. Clin. Invest.* **120**, 1561-1569.
Vokes, S. A., Ji, H., Wong, W. H. and McMahon, A. P. (2008). A genome-scale analysis of the cis-regulatory circuitry underlying sonic hedgehog-mediated patterning of the mammalian limb. *Genes Dev.* **22**, 2651-2663.
Wu, P., Jiang, T.-X., Shen, J.-Y., Widelitz, R. B. and Chuong, C.-M. (2006). Morphoregulation of avian beaks: comparative mapping of growth zone activities and morphological evolution. *Dev. Dyn.* **235**, 1400-1412.
Young, N. M., Chong, H. J., Hu, D., Hallgrimsson, B. and Marcucio, R. S. (2010). Quantitative analyses link modulation of sonic hedgehog signaling to continuous variation in facial growth and shape. *Development* **137**, 3405-3409.
Young, N. M., Hu, D., Lainoff, A. J., Smith, F. J., Diaz, R., Tucker, A. S., Trainor, P. A., Schneider, R. A., Hallgrimsson, B. and Marcucio, R. S. (2014). Embryonic bauplans and the developmental origins of facial diversity and constraint. *Development* **141**, 1059-1063.
Zhao, M., Qiao, M., Harris, S. E., Chen, D., Oyajobi, B. O. and Mundy, G. R. (2006). The zinc finger transcription factor Gli2 mediates bone morphogenetic protein 2 expression in osteoblasts in response to hedgehog signaling. *Mol. Cell. Biol.* **26**, 6197-6208.

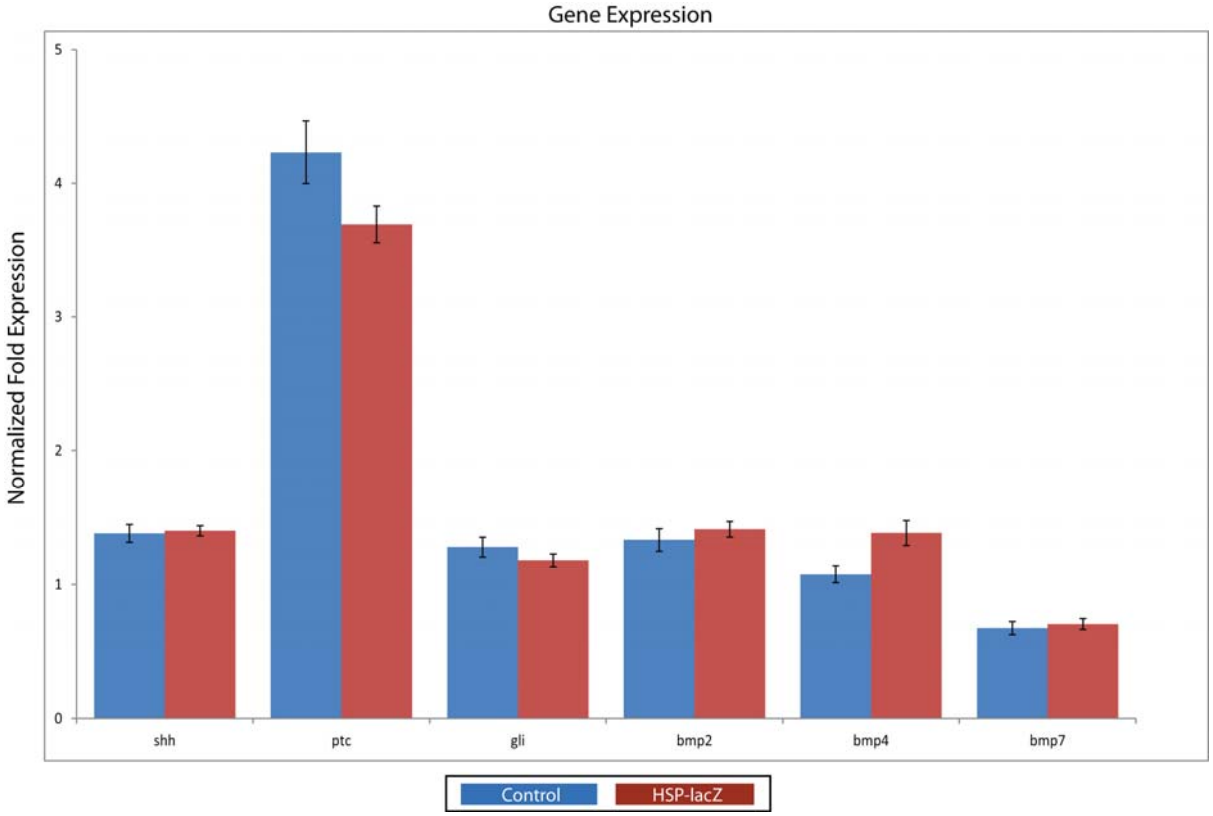

Figure S1. Gene expression is not altered by electroporation.

To control for changes in gene expression that may result from electroporation alone, embryos were electroporated with HSP-LacZ and then gene expression was analyzed 48 hours afterward. No changes in any genes in question were observed.

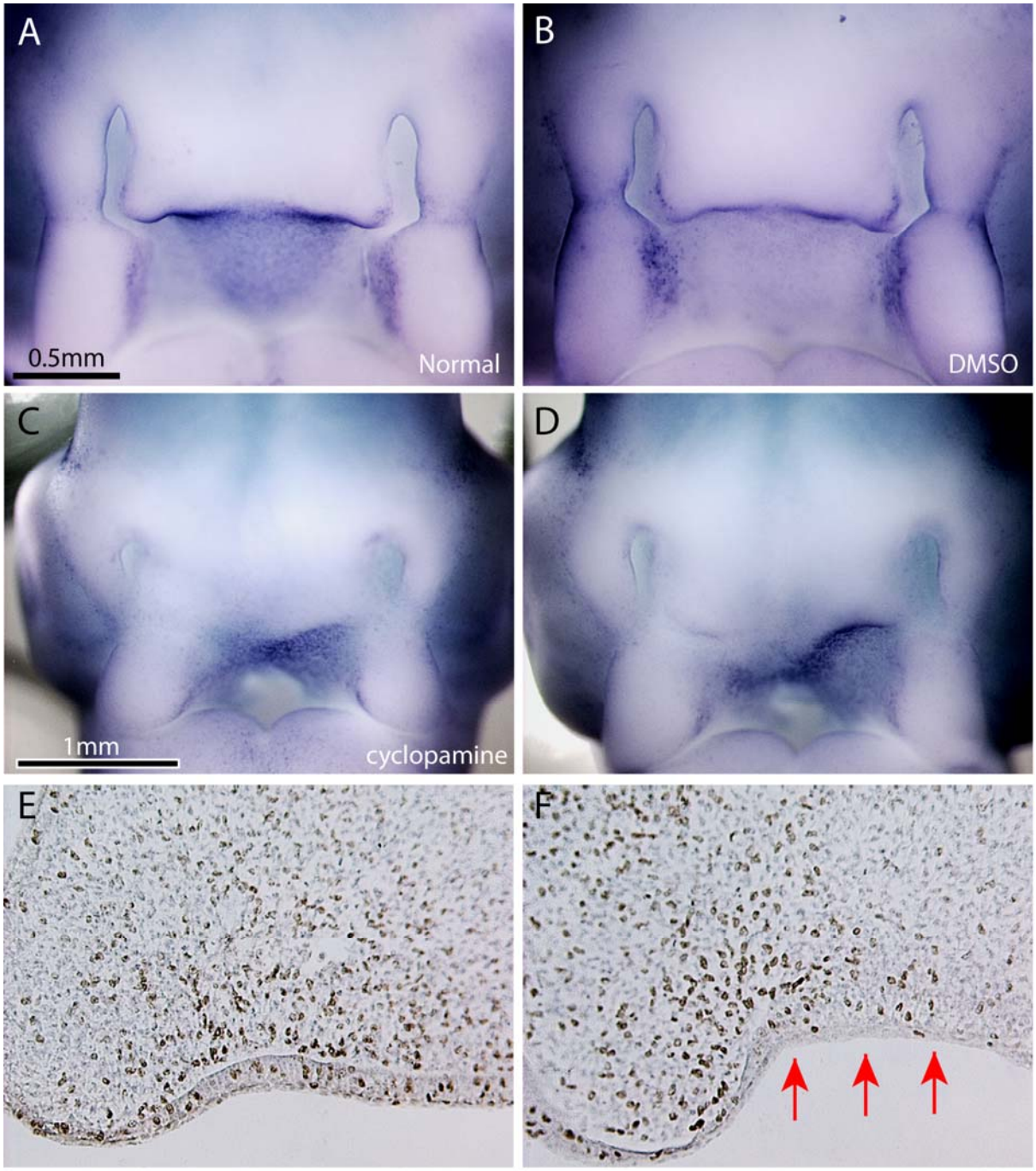

Figure S2. Cyclopamine and *Shh* expression.

(A) Normal and **(B)** control embryo illustrate the normal morphology and *Shh* expression. **(C,D)** After cyclopamine treatment the expansion of *Shh* is not observed on the treated side of the face. **(E)** Proliferation in a normal embryo. **(F)** Decreased proliferation is obvious after cyclopamine treatment (red arrows) similar to Fig. 2.

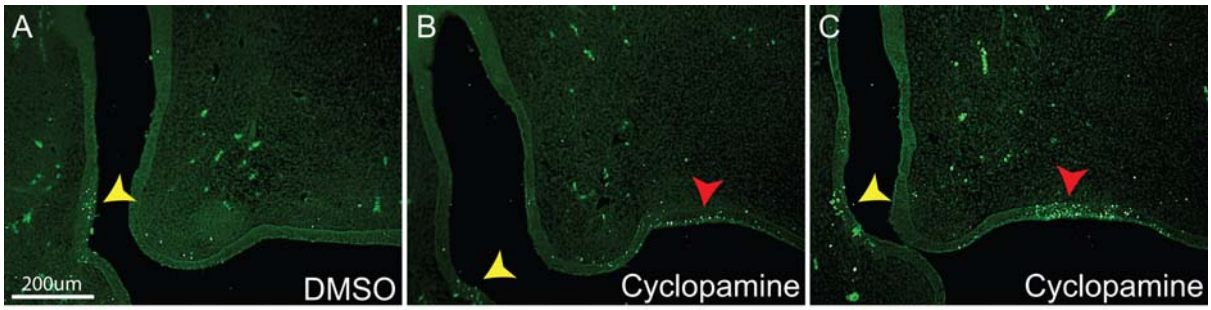

Figure S3. Cyclopamine and apoptosis.

(A) TUNEL staining in a control embryo exposed to DMSO shows few TUNEL positive cells. Programmed cell death in the lateral nasal process is evident (yellow arrow). **(B,C)** After cyclopamine treatment an increase in TUNEL positive cells were observed in the foci within the ectoderm (red arrow), but the epithelium remains intact and does not undergo widespread cell death.

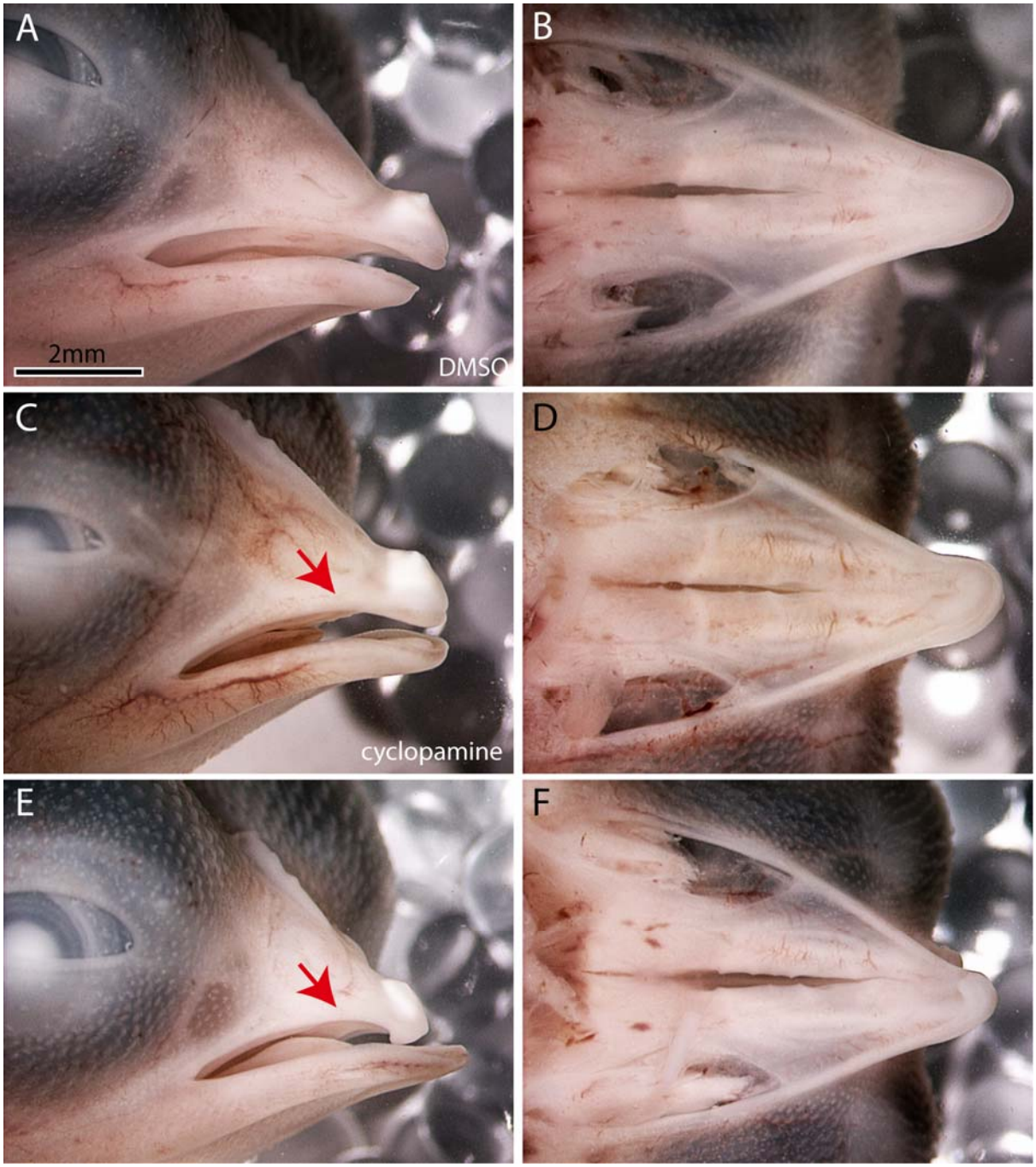

Figure S4. Cyclopamine and shape.

(A) Lateral and **(B)** dorsal view of a control embryo showing normal morphology of the upper jaw. **(C-F)** After cyclopamine treatment, a cleft in the upper jaw is evident (red arrows in C,E).

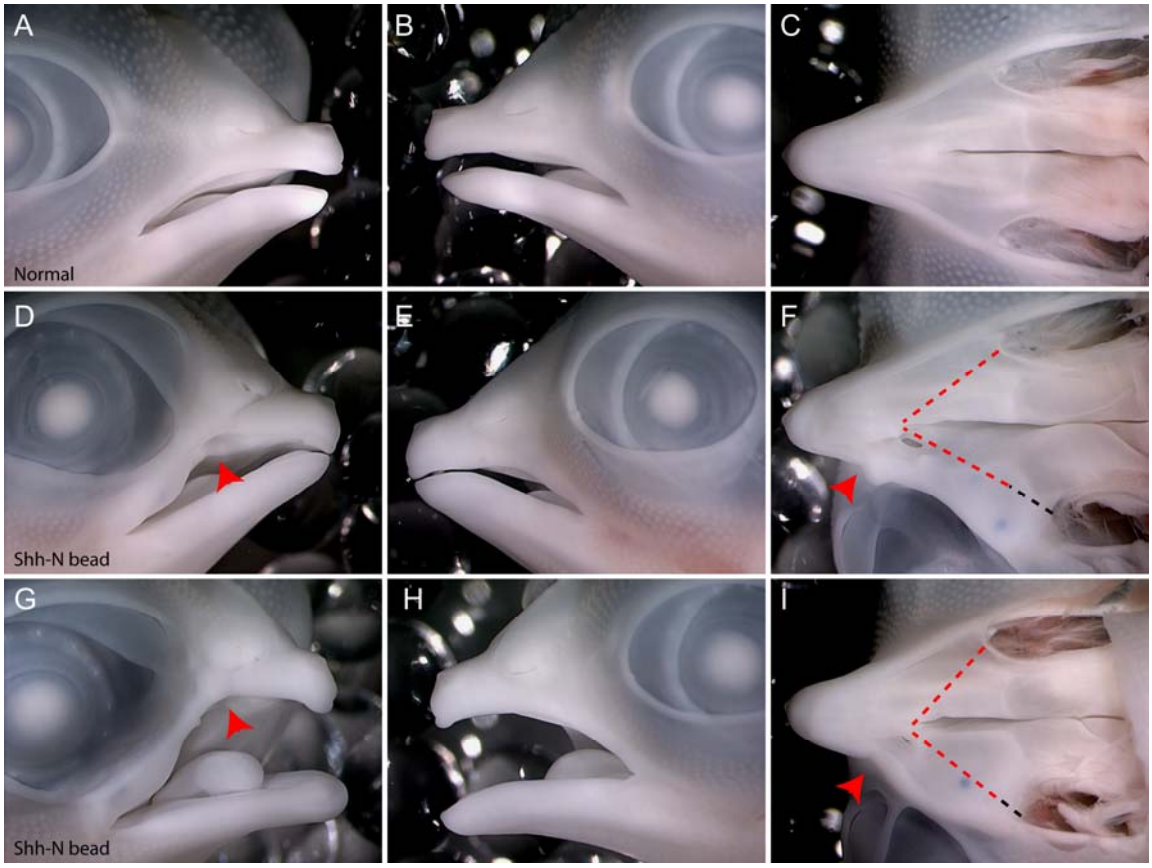

Figure S5. Activating SHH signaling leads to cleft palate.

(A) View of right and **(B)** left sides of a normal chick embryo at day 10. (**C**) Ventral view of the upper jaw in a normal embryo at day 10. (**D**) The right (treated) side of an embryo treated with a bead soaked in SHH-N illustrates a cleft (red arrowhead) of the primary palate. **(E)** The left (untreated) side appears unaffected. (**F**) Ventral view of the jaw of this treated embryo shows a cleft of the primary palate (arrowhead) as well as an increase in the gap of the palatal shelves. The red dotted line is the normal length of the upper jaw. The increase in size is shown by the red and black dotted line. (**G**) View of the right (treated) side of an embryo at day 10 shows a severe cleft (arrowhead), (**H**) while the left (untreated) side appears unaffected. **(I)** Ventral view of the upper jaw shows a cleft primary palate (arrowhead) and a widening of the space between the palatal shelves. The red dotted line is the normal length of the upper jaw. The increase in size is shown by the red and black dotted line.

Table S1. qPCR primers

GAPDH FW: CTGGTATGACAATGAGTTTGG
RV: ATCAGTTTCTATCAGCCTCTC

Shh FW: GCTGACAGACTGATGACTCA
RV: TCGTAGTGCAGCGATTCCTC

GLI1 FW: TGAAACAAACTGCTACTGGG
RV: ACACAAACTCCTTCTTCTCC

PTC FW: GCTTTCCTTTACTACAACTACCC
RV: GCAAGCATTAGTAAGTAGCCA

BMP2 FW: TTAACTTCCATCCCTAATGAGGAG
RV: ATGGTTAGGTTGTCCGTGT

Bmp4 FW: CCCAGTTACATGCTGGATC
RV: CTTCGTAAATGTTTATCCG

Bmp7 FW: AAAGCATAGATGGGCAAAGC
RV: GTCCCTGAAGCTGACATAGAG

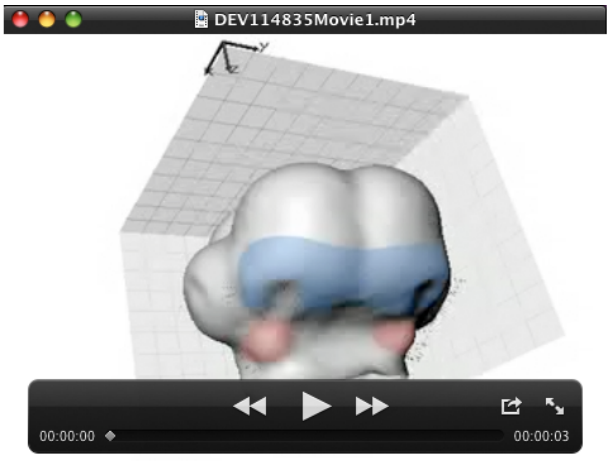

Movie 1. Growth of the upper jaw anlagen. A surface rendering is warped along PC1 (Fig. 1) to illustrate the growth pattern of the upper jaw anlagen from 90-160 h of development. The FNP is colored blue and the MxP is colored pink. During this time the FNP grows posteriorly and the MxP grows rostrally.